ISSN 2070-2051, Protection of Metals and Physical Chemistry of Surfaces, 2017, Vol. 53, No. 5, pp. 859–863. © Pleiades Publishing, Ltd., 2017.

NANOSCALE AND NANOSTRUCTURED MATERIALS AND COATINGS

# Hot Corrosion Behaviour of Plasma Sprayed Alumina + YSZ Particle Composite Coating[1]

**Muhammet Karabaş[a], Emre Bal[b, *], and Yılmaz Taptik[a]**

[a] *İstanbul Technical University, Department of Metallurgical and Materials Engineering, 34469, Istanbul, Turkey*

[b] *Akdeniz University, Vocational School of Technical Sciences, 07058, Antalya, Turkey*

**e-mail: emrebal@akdeniz.edu.tr*

Received March 17, 2016

**Abstract**—Hot corrosion is one of the damage mechanisms in thermal barrier coatings (TBCs) due to the molten salt effects as a result of combustion of low quality fuel. In this study, the hot corrosion behaviour of alumina – yttria stabilized zirconia particle composite coatings produced by thermal spraying for use as a thermal barriers on industrial gas turbines and in jet engines was evaluated. Plasma sprayed coatings with three different amounts of alumina- yttria stabilized zirconia particle composite have been exposed to 50 wt % $Na_2SO_4$ + 50 wt % $V_2O_5$ corrosive molten salt temperatures at 1050°C for 60 hours. Damages in the coatings surface and cross section after hot corrosion tests have been studied by using a scanning electron microscope to observe the microstructure and *x*-ray diffraction techniques to analyze the phase composition. The results have shown that the amount of $YVO_4$ crystals on the surface of YSZ coatings decrease while $Al_2O_3$ increases in YSZ + $Al_2O_3$ composition, therefore, the hot corrosion resistance of TBC improves with the addition of $Al_2O_3$.

*Keywords*: hot corrosion, plasma spray, thermal barrier coating

**DOI:** 10.1134/S2070205117050069

## 1. INTRODUCTION

Thermal Barrier Coatings (TBCs) is a technique which is largely applied as a protection shield against high temperatures for the structural components in stationary and aerospace gas turbines. The Thermal Barrier Coatings (TBCs) concept involves placing a MCrAlY bond coat (M = Ni, Co) as an oxidation resistance layer and top coat thermally insulating ceramic layer between a cooled metallic component and the hot working gas to reduce heat transfer to the component [1–5].

Hot corrosion is one of the most considerable damage mechanisms for the TBCs. Low quality fuels contain some corrosive contamination such as Na and V. These contaminations accumulate on the TBCs surface in the form of $Na_2SO_4$ and $V_2O_5$ salts. These salts, then, react with the yttria and cause phase transformation in the YSZ, which is a transition from tetragonal or cubic zirconia to monoclinic phase. This phase transformation leads to a volume expansion approximately 3–5% and cause damages in the TBCs such as cracks or spallation on TBCs surface [4–6, 16].

TBCs structure has porosity about 20–30%. Porosities about 20–30% improve thermal shock lifetime of TBCs. On the other hand, these porosities help the molten salts to be carried into the coating and enlarge contact area between coating and corrosive salts. Hence, low porosity TBCs Alumina has low oxygen diffusivity and it is not soluble in the YSZ. Addition of the alumina particles into the YSZ decreases the porosities in the TBC structure about the 10–15%. Moreover, Alumina particles in the YSZ cause a local compressive stress and hinder the phase transformation of zirconia and decelerate thermally grown oxide layer (TGO) growth [9, 14, 15].

Affrasiabi et al. studied the hot corrosion behaviour of the plasma-sprayed laminate and particle composite 40 wt % $Al_2O_3$ + YSZ coating which is exposed to molten $Na_2SO_4$ + $V_2O_5$ salts. They demonstrated that monoclinic $ZrO_2$ transformation from tetragonal $ZrO_2$ and $YVO_4$ crystals formation led to damages in the TBCs and monoclinic $ZrO_2$ fraction of YSZ +40 wt % $Al_2O_3$ particle composite coating was lower than usual YSZ [7].

In this study, the effects of $Al_2O_3$ addition into the YSZ on hot corrosion behavior of TBCs have been studied. In order to understand the effects of $Al_2O_3$ amount on hot corrosion behavior of $Al_2O_3$ + YSZ TBCs, 35 wt %, 50 wt %, 65 wt % $Al_2O_3$ + YSZ TBCs have been produced and hot corrosion tests have also been performed.

[1] The article is published in the original.

**Table 1.** Process parameters of HVOF

| Material | Pressure (bar) | | | Flow rate (SCFH) | | | Process | |
|---|---|---|---|---|---|---|---|---|
| AMDRY 997 | oxygen | propane | air | oxygen | propane | air | spray distance, mm | powder feed rate, g/min |
| | 10.3 | 6.2 | 7.2 | 24 | 40 | 50 | 250 | 50 |

## 2. EXPERIMENTAL METHODS

### *2.1. Materials and Coatings*

316L stainless steel disk-shaped samples with the diameter of 25.4 mm and with the thicknesses of 2 mm have been used as substrate. Prior to bond coat production, the substrate was grit-blasted by using 50–80 grain mesh alumina particles in order to remove surface oxides and improve adhesion of bond coat. Commercial Sulzer Metco Amdry 997 (Ni–23Co–20Cr–8.5Al–4Ta–0.6Y) powder was selected to manufacture the bond coats. The spray torches (APS and HVOF gun) were fastened on a three-axis CNC table and gun speed was selected as 600 mm/min. Grit-blasted samples were clamped on the turntable and turntable speed has been selected as 100 rpm and a number of passes was selected to be 12. Amdry 997 bond coat powder was coated by using DJ2700 HVOF gun. HVOF process parameters are listed in Table 1.

Commercial Sulzer Metco 204NS ($ZrO_2$–8 wt % $Y_2O_3$) and Sulzer Metco 101NS ($Al_2O_3$) powders were selected for top coat materials. YSZ + 35, 50 and 65 wt % $Al_2O_3$ powders and ethanol were added in plastic bottle and it was mixed by using Turbula for 4 h. Then, mixed powders have been dried in incubator.

Three different coatings have been produced by air plasma spray (APS) method by using Sulzer Metco 9MB plasma spray gun. Gun nozzle was a commercial Sulzer Metco 730C and powder injection angle was perpendicular to plasma flame. Process parameters of plasma spraying are listed in Table 2.

### *2.2. Hot Corrosion Tests*

$V_2O_5$ and $Na_2SO_4$ powders were selected as corrosive salts. 50 wt % $V_2O_5$ and 50 wt.% $Na_2SO_4$ salts were mixed in turbula for 2 h. The corrosive salt with a concentration of 30 mg/cm$^2$ was spread over the surface coatings leaving 3 mm distance from the edge to avoid edge effect. The samples were heated up to 1050°C and held for 60 h in an electric furnace with air atmosphere, then allowed to cool down inside the furnace.

**Table 2.** Process parameters of plasma spray

| Paramaters | |
|---|---|
| Current, A | 500 |
| Primary gas, Ar (scfh) | 90 |
| Secondary gas, $H_2$ (scfh) | 15 |
| Carrier gas flow rate, Ar (scfh) | 13.5 |
| Number of passes | 6 |
| Spray distance, mm | 75 |
| Gun speed, mm/min | 200 |
| Turntable speed, rpm | 100 |

### *2.3. Microstructure and Chemical Analysis*

Microstructure, morphology and chemical composition of the surface and the cross-section of the coatings have been examined by field emission electron microscopy (JEOL JSM 7000F) equipped with EDS. X-ray diffraction (Rigaku Miniflex) has been used to determine the crystalline structure of the coatings and hot corrosion products.

## 3. RESULTS AND DISCUSSIONS

### *3.1. Microstructure and Crystalline Structure of the Coatings Before Hot Corrosion Tests*

Figure 1 shows the cross-sections of the three different TBCs. In Fig. 1 are shown 35 wt % $Al_2O_3$ + YSZ, 50 wt % $Al_2O_3$ + YSZ and 65 wt % $Al_2O_3$ + YSZ, respectively, which includes the bond coat and top coat layers. Thickness of bond coats was measured approximately to be 100 μm and top coats of the three sample groups measured approximately to be 150, 180, 200 μm, respectively. The dark area in the top coats is YSZ and light area is shown to be $Al_2O_3$. The addition of $Al_2O_3$ into the YSZ led to decreasing of percentage of porosity in the top coat.

When the distribution of alumina in the ceramic top layer is examined, it seems that alumina particles distributed randomly, but top coating surface contains less alumina particles than the inner layer.

The XRD analysis has been carried out on the surface of the coatings before hot corrosion tests. Figure 2 illustrates the XRD patterns of sprayed as YSZ + $Al_2O_3$. TBCs contain tetragonal phase of $ZrO_2$, rhombohedral α $Al_2O_3$ and orthorhombic δ $Al_2O_3$ phases.

### *3.2. Microstructure and Crystalline Structure of the Coatings After Hot Corrosion Tests*

Figure 3 shows SEM micrographs of the three different TBCs surface after hot corrosion tests. All TBCs have a porous surface structure. However; while the amount of alumina in the top coating increases, the

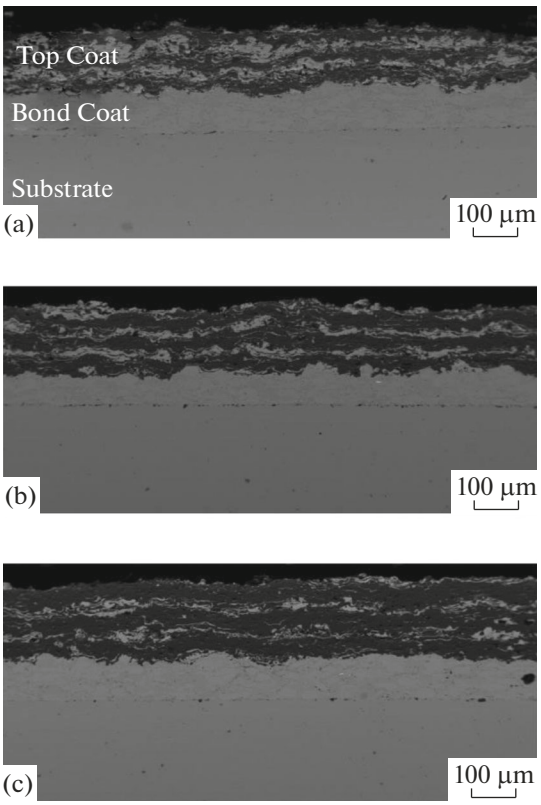


**Fig. 1.** Cross-sectional SEM images of the as sprayed TBCs: (a) YSZ + 35 wt % $Al_2O_3$; (b) YSZ+50 wt % $Al_2O_3$; and (c) YSZ + 65 wt % $Al_2O_3$.

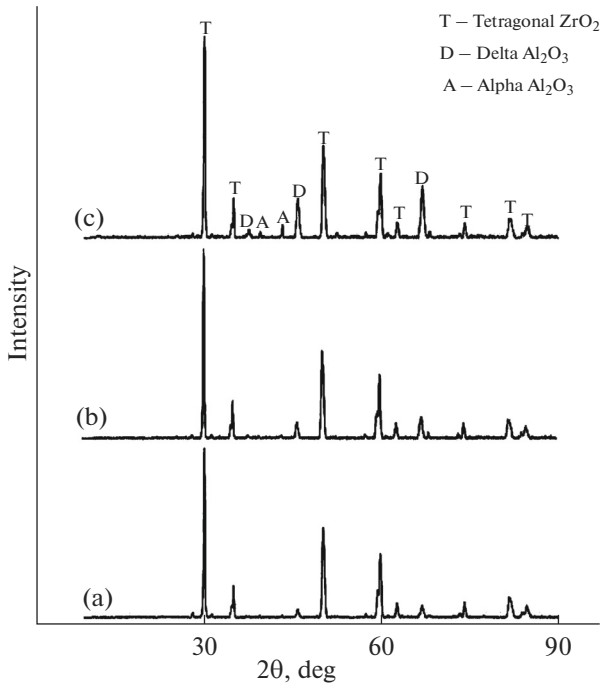


**Fig. 2.** XRD patterns of the as sprayed YSZ + $Al_2O_3$ TBCs: (a) YSZ + 35 wt % $Al_2O_3$; (b) YSZ + 50 wt % $Al_2O_3$; and (c) YSZ + 65 wt % $Al_2O_3$.

area fraction of porous structure in the coating layer reduces. In this case, the penetration of corrosion product into the inner layer of TBCs proves to be difficult. As a result of 60-hour hot corrosion test $YVO_4$ forms which is shown in Fig. 3. $YVO_4$ has grown as rectangular columnar rod shape on the TBCs surface. With increasing alumina content in the top coat caused the suppression of growing $YVO_4$ and finally decreased the amount of corrosion product on the TBCs surfaces.

Figure 4 illustrates the cross-sectional SEM images of YSZ + $Al_2O_3$ TBCs after hot corrosion tests. The separation of TBCs containing 50 and 65% $Al_2O_3$ from the surface was observed between the bond coat and the top coat. On the other hand, as a result of corrosion tests and sintering effect, microstructure of TBCs underwent a severe deformation. After the tests, porosities for 50 and 65% $Al_2O_3$ groups were no longer observed on the cross-sectional SEM micrographs. However, porosities in 35% $Al_2O_3$ group were still observed, but much less than pre-test phase when compared.

As is seen in Fig. 5, according to the XRD patterns of TBCs after hot corrosion test, all of tetragonal zirconia phases transformed into monoclinic zirconia.

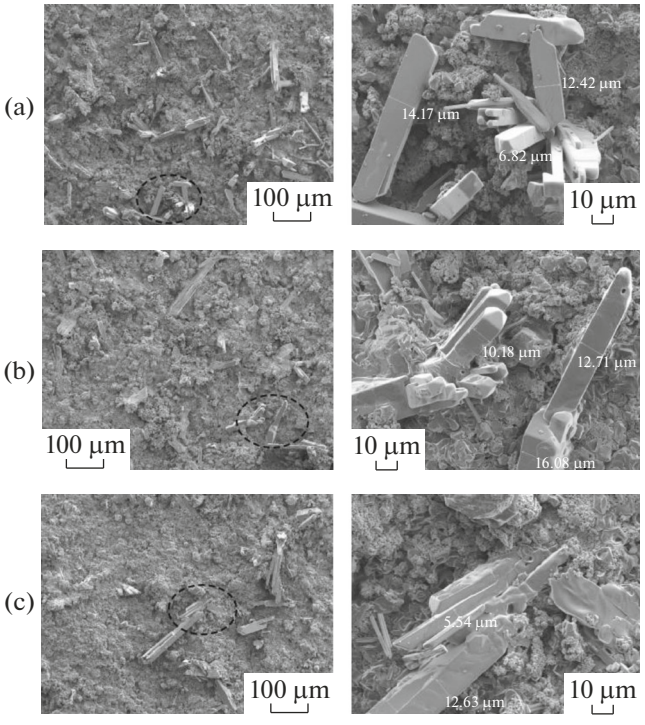


**Fig. 3.** SEM micrographs of the TBCs surface after hot corrosion: (a) YSZ + 35 wt % $Al_2O_3$; (b) YSZ + 50 wt % $Al_2O_3$; and (c) YSZ + 65 wt % $Al_2O_3$.

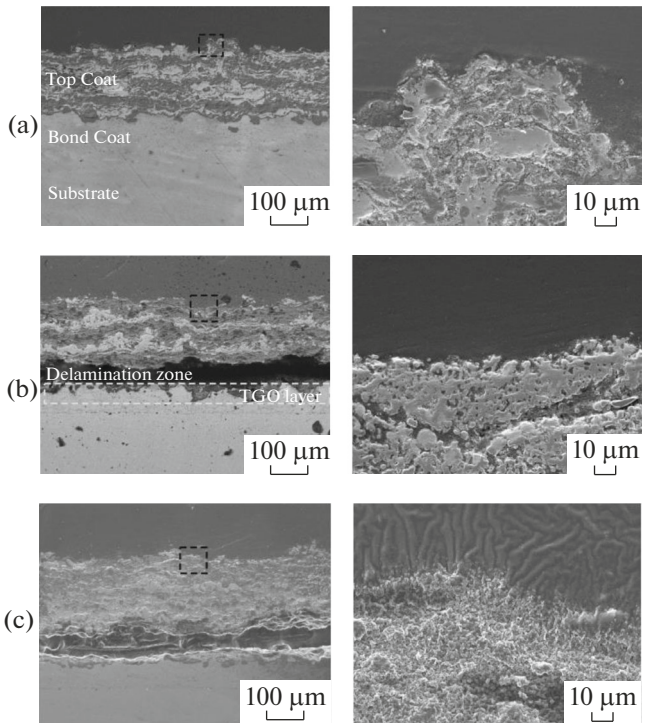


**Fig. 4.** Cross-sectional SEM images of the TBCs after hot corrosion tests: (a) YSZ + 35 wt % $Al_2O_3$; (b) YSZ + 50 wt % $Al_2O_3$; and (c) YSZ + 65 wt % $Al_2O_3$.

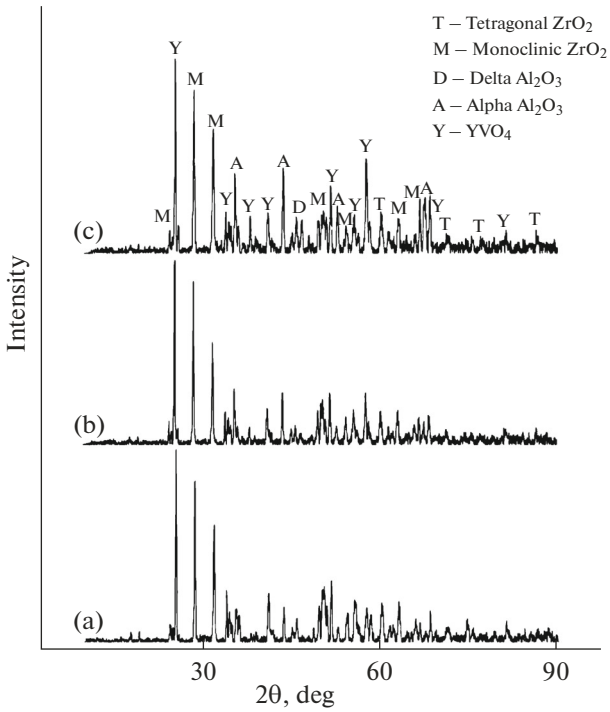


**Fig. 5.** XRD patterns of the YSZ + $Al_2O_3$ TBCs after hot corrosion tests: (a) YSZ + 35 wt % $Al_2O_3$; (b) YSZ + 50 wt % $Al_2O_3$; and (c) YSZ + 65 wt % $Al_2O_3$.

The mechanism of tetragonal-monoclinic zirconia phase transformation during hot corrosion tests can be explained by following reactions [10]:

$$V_2O_5 + Na_2SO_4 \rightarrow 2(NaVO_3) + SO_3, \quad (1)$$

$$ZrO_2(Y_2O_3) + 2(NaVO_3) \rightarrow ZrO_2(\text{monoclinic}) + 2YVO_4 + Na_2O. \quad (2)$$

Firstly, as it is seen in Eq. (1), sodium vanadate ($NaVO_3$) is formed, then, according to Eq. (2), $NaVO_3$ reacts with yittria ($Y_2O_3$) and causes the destabilization of tetragonal zirconia. Eventually, tetragonal $ZrO_2$ transforms to monoclinic $ZrO_2$ and forms $YVO_4$ and $Na_2O$. It is assumed that, the $Na_2O$ compound sublimated during hot corrosion test (Eq. (2)). According to previous researches [7, 12, 13] Na was detected on hot corrosion of plasma sprayed $Al_2O_3$ and $ZrO_2$ coatings in molten $Na_2SO_4$, and the following reactions were suggested:

$$Na_2SO_4 \rightarrow Na_2O + SO_3, \quad (3)$$

$$Al_2O_3 + Na_2O \rightarrow 2NaAlO_2, \quad (4)$$

On the surface of $Al_2O_3$ particles, $NaAlO_2$ can be formed because the hot corrosion rate of $ZrO_2$ coating in molten $Na_2SO_4$ is much higher than the $Al_2O_3$ coating. In this study, $NaAlO_2$ was not detected by XRD analysis, so, it cannot be assumed that during hot corrosion, $NaAlO_2$ compound protects $Al_2O_3$ layer [7, 10, 11].

In order to find out how deep corrosion salts penetrate, EDS line scan analysis was applied throughout surface along cross-section of the coating. Figure 6 shows the EDS line scan results of the three different TBCs.

While vanadium concentration is much higher on the surface and close areas of the coating surface, it gets less and less towards inner layers. But the concentration change in Na and S is very close to each other throughout coating. Capillary cracks among the splats and micro porosities existing in the coating led to the penetration of the hot corrosion salts towards the inner sides of the coating.

When V concentration is examined based on Figure 6, it exists less in inner sections than the outer sections because it encounters an $Al_2O_3$ barrier and this confines its penetration into the deep sections of the coating.

When the EDS line scan results of three different coatings are examined, as far as their amounts are concerned, sodium and sulphur have dispersed very closely throughout the cross-section of the three coatings. Melting $Na_2SO_4$ salts haven't disintegrated in non-$Al_2O_3$ regions but they have dispersed in the coating through melting.

## 4. CONCLUSIONS

Monoclinic $ZrO_2$ and $YVO_4$ crystals formed as a result of reaction of molten salt containing $V_2O_5$ with

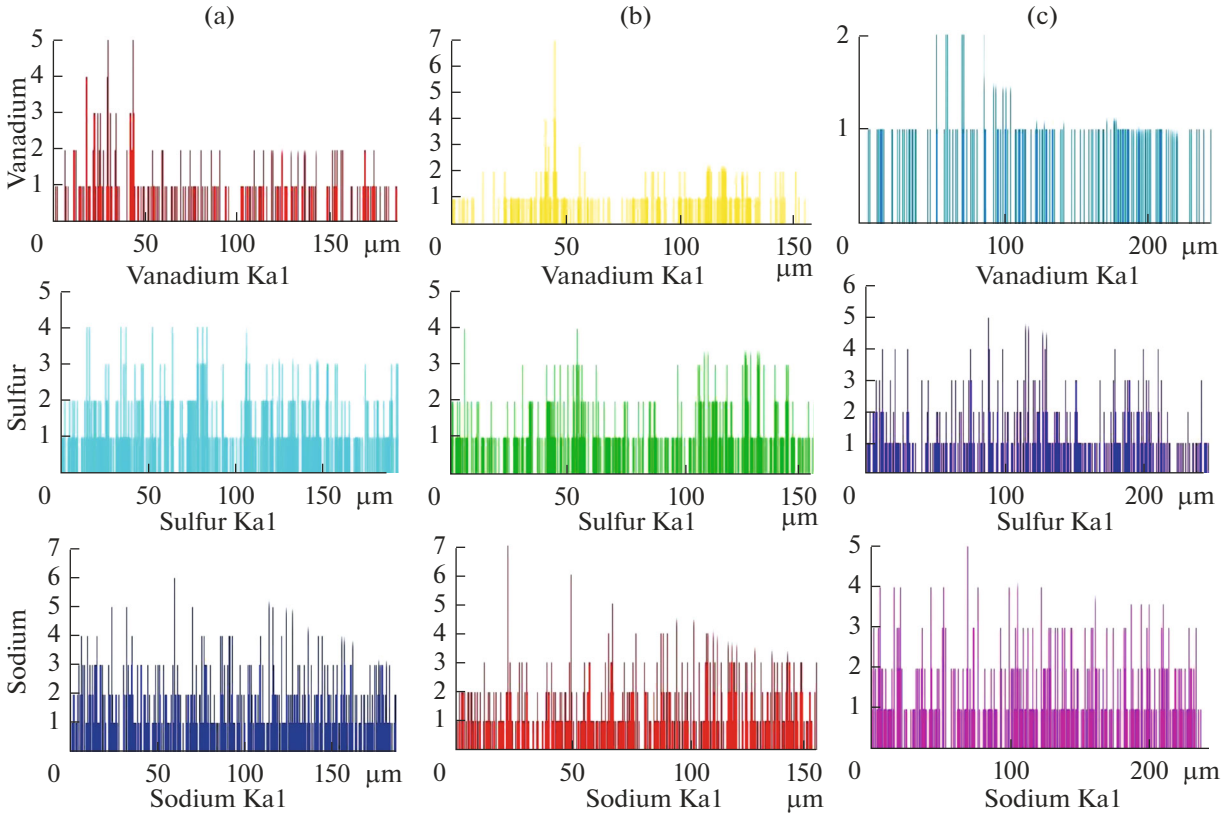


**Fig. 6.** EDS line scan results of: (a) YSZ + 35 wt % $Al_2O_3$; (b) YSZ + 50 wt % $Al_2O_3$; and (c) YSZ + 65 wt % $Al_2O_3$.

$Y_2O_3$. The formation of monoclinic $ZrO_2$ and $YVO_4$ crystals, as hot corrosion products, caused the failure of TBCs.

Amount of $YVO_4$ crystals on the surface of YSZ coatings decreases with the increase of $Al_2O_3$ in YSZ + $Al_2O_3$ composition.

YSZ + 65 wt % $Al_2O_3$ seems to be the most resistant coating during exposure to hot corrosion. This is because YSZ + 65 wt %$Al_2O_3$ has more dense alumina layer than that of YSZ + 50 wt % $Al_2O_3$ and YSZ + 35 wt % $Al_2O_3$ which significantly prevented the infiltration of molten salt ($V_2O_5$ + $Na_2SO_4$) into YSZ layer.

According to this study, with increasing alumina addition (up to 65%) into YSZ composition, hot corrosion resistance of TBC improves.

## ACKNOWLEDGMENTS

We would like to thank to Mr. Hüseyin YİĞİT at Akdeniz University for his kind support.

## REFERENCES

1. Herman, R.B., *Plasma-Spray Coating, Principles and Applications,* Weinheim, New York, Basel, Cambridge, Tokyo: VCH, 1996, p. 100.
2. Matejka, D. and Benko, B., *Plasma Spraying of Metallic and Ceramic Materials,* New York: John Wiley & Sons, 1989, p. 11.
3. *Handbook of Thermal Spray Technology,* Davis, J.R., Ed., Materials Park, OH: ASM Int., 2004, p. 1.
4. Jones, R.L., *J. Therm. Spray Technol.,* 1997, vol. 6, no. 1, p. 77.
5. Karabas, M., Bal, E., Kilic, A., and Taptik, Y., *J. Aust. Ceram. Soc.,* 2016, vol. 52, no. 2, p. 175.
6. Bal, E., Karabaş, M., and Taptık, Y., *Proc. 25th IRES Int. Conference,* India, 2016, p. 17.
7. Afrasiabi, A., Saremi, M., and Kobayashi, A., *Mater. Sci. Eng., A,* 2008, vol. 478, p. 264.
8. Parka, S.Y., Kima, J.H., Kimb, M.C., et al., *Surf. Coat. Technol.,* 2005, vol. 190, p. 357.
9. Karaoglanli, A.C., Altuncu, E., Ozdemir, I., et al., *Surf. Coat. Technol.,* 2011, vol. 205, p. 369.
10. Gurrappa, I., *J. Mater. Sci. Lett.,* 1998, vol. 17, p. 1267.
11. Batista, C., Portinha, A., Ribeiro, R., et al., *Surf. Coat. Technol.,* 2006, vol. 200, p. 6783.
12. Chen, Z., Wu, N.Q., Singh, J., and Mao, S.X., *Thin Solid Films,* 2003, vol. 443, p. 46.
13. Chen, H.C., Liu, Z.Y., and Chuang, Y.C., *Thin Solid Films,* 1992, vol. 223, p. 56.
14. Keyvani, A., Saremi, M., and Sohi, M.H., *J. Alloys Compd.,* 2011, vol. 509, p. 8370.
15. Keyvani, A., Saremi, M., Sohi, M., et al., *J. Alloys Compd.,* 2014, vol. 600, p. 151.
16. Keyvani, A., Saremi, M., and Sohi, M.H., *J. Alloys Compd.,* 2010, vol. 506, p. 103.